SUPPLEMENTAL MATERIAL

Supplemental Methods

Mice

The Tsukuba University Ethics Committees for Animal Experiments approved all experiments. MGTH2A mice, conditional transgenic mice expressing *Mef2c/Gata4/Tbx5/Hand2* (MGTH) separated by 2A peptides (MGTH2A) under the CAG promoter with Cre expression, were generated as described previously.[14] B6.Cg-Gt(ROSA)26Sortm14(CAG-tdTomato)Hze/J (R26R-tdTomato; JAX stock No. 007914) mice were purchased from the Jackson Laboratory. Tcf21^{iCre} mice were obtained from Dr. Eric Olson. The conditional knock-in single-factor-expressing mice (G, M, T, and H) were generated at the Laboratory Animal Resource Center at the University of Tsukuba (Ibaraki, Japan) using plasmids with a Rosa-CAG-LSL-Z structure. Both ends of this construction link to the Rosa26 homologous sequence,[39] and LSL is a cassette with three aligned simian virus 40 polyadenylations (SV40pA) sequences flanked by loxP sites. Plasmids with G, M, T, and H full-length coding sequences inserted into the Z site of CAG-LSL-Z were constructed. The constructed plasmids were purified and introduced into ICR mouse embryos with CRISPR-Cas9 effectors.[40] Each gene sequence was inserted into the Rosa26 locus by homology-directed repair. The inserted gene was introduced into Rosa26, and gene insertion into other loci was confirmed using DNA PCR using the listed primers (Table S3). Mice with gene insertion only at the target Rosa26 locus were selected. F0 mice were mated with the ICR mice purchased from CLEA Japan (Tokyo, Japan) to obtain F1 offspring. Tcf21i^{Cre}/Tomato mice were generated by crossing Tcf21^{iCre} mice and tdTomato mice.[17,41] MGTH2A mice and SF-G mice were crossed with Tcf21^{iCre}/Tomato mice to generate Tcf21^{iCre}/Tomato/MGTH2A triple transgenic mice and Tcf21^{iCre}/Tomato/SF-G triple transgenic mice, respectively.[14] SF-G, M mice were mated with Tcf21^{iCre} and crossed to produce double-transgenic mice. These transgenic mice were maintained on a mixed background (ICR and

C57BL/6J) and identified using standard PCR with the listed primers (Table S3). Throughout the mating and experimental period, mice were maintained under specific pathogen-free (SPF) conditions at the Experimental Animal Resource Centre, University of Tsukuba (Ibaraki, Japan). All mice were subjected to at least one month of acclimatization prior to initiating *in vivo* experiments. No immune deficiencies or other health problems were observed in the transgenic mice, and all animals were naïve to experimental assessment and drug treatment before use. All animals were group-housed and bred in a dedicated SPF facility with 12 h/12 h light-dark cycles, had *ad libitum* access to food and water, and were checked daily. Their health status was routinely checked to maintain SPF grades. The study design for each *in vivo* experiment is described in Table S1 according to the ARRIVE guidelines (https://arriveguidelines.org/).

HFpEF model generation

Experiments were performed using male adult (10- to 12-week-old) mice. HFpEF was induced by feeding a high-fat diet (HFD; HFD32; Nippon Crea, Tokyo, Japan) and providing drinking water containing L-NAME (1.0 g/L, pH 7.4 NaOH; N5751; Sigma, St. Louis, MO, USA) as described previously.[18] The number of animals used was determined based on our pilot experiments with this model. The mice were monitored for an appropriate duration, and only healthy individuals without hair loss or bite wounds were included in the study. Randomization was performed after genotyping. Both HFD and L-NAME dissolved in water were replaced every three days. Control mice were fed normal chow (Oriental Yeast) and provided water. No deaths or exclusions were noted in this study. Two different investigators were involved for each animal, with the protocol described as follows: a first investigator (TS) administered the treatment based on the randomization table. This investigator was the only individual aware of the treatment group allocation. A second investigator (YY) was responsible for the surgical procedure and measurements.

Tamoxifen (TAM) administration

Mice were administered TAM (T5648; Sigma) intraperitoneally at a dose of 2 mg/day for five consecutive days. TAM was dissolved in peanut oil (90%; P2144; Sigma) and ethanol (10%) at a concentration of 50 mg/mL.

BrdU assay

BrdU (Sigma, B5002) was dissolved in phosphate-buffered saline (PBS; 10 mg/ml). In the experiment depicted in Figures S2A-B, the initial BrdU dose was administered intraperitoneally (1 mg) five weeks after TAM administration. Subsequently, BrdU-supplemented water (1 mg/mL) was provided until the end of the analysis (10 weeks after TAM administration). In the experiment depicted in Figures S9A-B, 1 mg of BrdU was administered intraperitoneally one week after TAM administration, with BrdU-supplemented water (1 mg/mL) supplied until the end of the analysis (five weeks post-TAM administration). The BrdU-supplemented water was refreshed every three days.

Echocardiography

The transthoracic echocardiographic imaging of mice was performed using Vevo 2100 (Visual Sonics) with an MS550S Transducer (32–56 MHz, Visual Sonics) at the beginning of the experiment and every five weeks thereafter. Mice were anesthetized with 4% isoflurane, maintained under 1–2% isoflurane, and supplied with 1 L/min of oxygen. The testing order was randomized daily. During echocardiographic imaging, body temperature was controlled with a warming pad, while electrocardiogram monitoring was performed using limb electrodes. Echocardiographic imaging was analyzed using Vevo LAB (version 3.1.1, Visual Sonics). Anterior wall thickness, inner diameter, and posterior wall thickness of the left ventricle at end-

diastole were measured by M-mode echo at the papillary muscle level in the left ventricular short-axis image. Left ventricular ejection fraction (LVEF) was measured in B-mode using a parasternal long-axis view as follows: Initially, the left ventricular end-diastolic area (LVEDA) and end-systolic area (LVESA) were obtained by tracing the endocardial boundary of the left ventricular cavity at both end-systole and end-diastole, respectively. Next, the left ventricular lengths were measured at end-diastole (left ventricular end-diastolic length [LVEDL]) and end-systole (left ventricular end-systolic length [LVESL]), respectively. LVEF was calculated by determining LVEDV and LVESV using the following equations[42]:

$LVEDV = 8 \times LVEDA^2 / (3\pi \times LVEDL)$,

$LVESV = 8 \times LVESA^2 / (3\pi \times LVESL)$,

$LVEF = (LVEDV - LVESV) / LVEDV) \times 100$

Diastolic function was assessed by measuring the E/A and E/E' ratios from the apical four-chamber view. E and A waves were measured in a pulsed-wave Doppler mode between mitral valve leaflets. S' and E' waves were measured in tissue Doppler mode at the peak systolic motion and early diastolic motion velocity of the mitral annulus, respectively. All measurements were obtained from at least three cardiac cycles, and the means of the results were used for the analysis.

Blood pressure recordings

The blood pressure of the mice was measured noninvasively under conscious conditions using a mouse tail-cuff measuring device (CODA, Kent Scientific, Torrington, CT, USA). Mice were placed in individual holders on a temperature-controlled platform (37°C), and recordings were obtained under steady-state conditions. Before testing, all mice were trained to acclimatize to short-term restraints. Blood pressure measurements were performed every five weeks, and the average of multiple measurements was obtained at each time point. The testing order was

randomized daily.

Hemodynamic assessment

The mice were anesthetized with 3% isoflurane and mechanically ventilated (SN-480-7; Shinano, Tokyo, Japan) with a maintenance dose of 1.5% isoflurane after endotracheal intubation. Their heart rate and electrocardiograms were continuously monitored on a warming pad during the experiment period. Before making an incision for invasive hemodynamic assessment, 0.5% lidocaine (AstraZeneca, Osaka, Japan) was applied locally as an analgesic, with the total dose not exceeding 7 mg/kg. The testing order was randomized daily. As described in a previous study, cardiac catheterization was performed using a mouse conductance catheter (SPR-839, Millar, Houston, TX, USA) and a Pressure-Volume System (MPVS-400, Millar).[43] The right internal carotid artery was exposed via an incision, and a conductance catheter was inserted. The tip was inserted into the left ventricle, and the left ventricular intraventricular pressure waveform in a stable state was recorded. Next, a small incision was made in the upper abdomen to identify the inferior vena cava. The pressure-volume (PV) loop waveform during inferior vena cava occlusion was recorded by applying pressure to the inferior vena cava with a cotton swab during a ventilation pause. Subsequently, parallel conductance (Vp) was determined by injecting 10 μL of 15% saline solution into the inferior vena cava to establish the Vp of the blood pool. The derived Vp was used to correct the PV loop data. Analysis was performed using the LabChart version 8.1.13 (ADInstruments, Sydney, Australia). Left ventricular end-diastolic pressure was calculated as the average of 10 cardiac cycles during the stable state before the abdominal incision. Saline correction and PV loop analysis were performed using the PV loop Workflow module in LabChart with default settings. After PV loop correction with saline calibration, the end-diastolic pressure-volume relationship was calculated using the waveform during the inferior vena cava compression.

Exercise exhaustion test

The mouse treadmill used a belt-type forced running machine (TMS-4N, MELQUEST). After two days of acclimatization to the treadmill, the mice ran at a warm-up speed of 5 m/min for 4 min at a 20° uphill incline. The speed was then increased to 14 m/min for 2 min. Subsequently, the speed was increased by 2 m/min every 2 min until the mice reached exhaustion, and the total running distance was measured. Exhaustion was defined as the inability to resume running within 10 s after contact with the electrical stimulation grid. The testing order was randomized daily.

Fluorescence-activated cell sorting analysis for *in vitro* studies

Cells were fixed in 4% paraformaldehyde (PFA) for 15 min, permeabilized with saponin (47036-250G-F; Sigma Aldrich, St. Louis, MO, USA), stained with anti-cTnT antibody (MS-295-P1; ThermoFisher Scientific, Waltham, MA, USA), and incubated with a secondary antibody conjugated with Alexa Fluor 488 (A11001; Invitrogen, Waltham, MA, USA) to detect cTnT expression using fluorescence-activated cell sorting (FACS). The cells were then analyzed using a FACS instrument (CytoFLEX S; Beckman Coulter, Brea, CA, USA) and the FlowJo software (Tomy Digital Biology, Tokyo, Japan).

Histology

Hearts were perfusion-fixed in 0.4% PFA after mice were euthanized by CO_2 inhalation. The hearts were quickly harvested and fixed overnight in 4% PFA. For immunostaining of frozen sections, frozen blocks were prepared in liquid nitrogen by embedding them in optimal cutting temperature compound after replacement with 20% sucrose solution. The hearts were cut vertically into 7-µm sections to expose both ventricles. Sections were stained with primary

antibodies against α-actinin (1:800, A7811; Sigma), BrdU (1:100, ab6326; Abcam), CD45 (1:25, 30F-11; Santa Cruz), and Postn (1:50, NBP1-30042; Novus, Centennial, CO, USA), followed by secondary antibodies conjugated with Alexa 488 (1:200, A11001; Invitrogen) and DAPI (D1306; Invitrogen). TUNEL staining was performed using the In Situ Cell Death Detection Kit, Fluorescein (11684795910, Roche), according to the manufacturer's instructions. Confocal microscopy was performed using an LSM800 microscope (Carl Zeiss, Baden-Württemberg, Germany), and Z-stack images were collected according to the standard protocol. The ratio of α-actinin$^+$/Tomato$^+$ cells and the relative frequency of induced cardiomyocytes (iCMs) with sarcomere structure were measured by counting 10 randomly selected fields from more than five sections in each mouse. Postn$^+$ area measurements were performed using the ImageJ software (National Institutes of Health, Bethesda, MD). The Postn$^+$ area, the ratio of BrdU$^+$/Tomato$^+$ cells, the ratio of Tunel$^+$/Tomato$^+$ cells, and the number of CD45$^+$ cells were measured in at least five randomly selected fields from three different sections of each mouse. All measurements and calculations were performed under blinded conditions.

Cardiomyocyte (CM) size, fibrosis area, vessel diameter, and capillary density determination

Paraffin sections were subjected to wheat germ agglutinin (WGA), Sirius red (SR), hematoxylin-eosin (HE), and Isolectin staining to measure CM cross-sectional area (CSA), fibrosis area, vessel diameter, and capillary density. After mice were euthanized by CO^2 inhalation, their hearts were perfusion-fixed in 0.4% PFA and then quickly removed and further fixed overnight in 4% PFA with 30 mM KCl (163-03545; FUJIFILM Wako Chemicals, Osaka, Japan). For immunostaining, WGA Alexa 488 conjugated (1:100, W11261; Invitrogen), Isolectin GS-IB4 Alexa 488 conjugated (1:100, I21411; Invitrogen), and DAPI (D1306; Invitrogen) were used. CM CSA and fibrosis area measurements were performed using ImageJ

(NIH). CM CSA was measured using at least 100 CMs for each mouse. The fibrosis area and capillary density were the mean values measured in at least 10 randomly selected fields from three different sections for each mouse. Vessel diameter was defined as the average of the long and short inner diameters of vessels with a lumen diameter of >100 μm in HE-stained sections of the LV. Measurements were obtained from five randomly selected fields from three different sections and were evaluated relative to the vessel diameter of the Ctrl-Chow. All measurements and calculations were performed under blinded conditions.

Reverse transcription-quantitative PCR (RT-qPCR)

For *in vivo* experiments, mice were euthanized by CO_2 inhalation, and their hearts were harvested immediately. Total RNA was extracted from fibroblasts, ventricles, and Tomato$^+$ cells isolated from the hearts using standard protocols. RT-qPCR was performed using the StepOnePlus Real-Time PCR system with primers listed in Table S2 and TaqMan probes (Applied Biosystems, Waltham, MA, USA). Target mRNA expression was corrected using *Gadph* expression.

RNA-sequencing

Total RNA was extracted from the whole ventricles of the three groups (Ctrl-chow, Ctrl-HFpEF, and TTg-HFpEF; n=3 each) at 15 weeks. After rRNA-depletion (E6310; NEB, Ipswich, MA, USA) and directed library synthesis (E7420; NEB), sequencing was performed using an Illumina NextSeq500. FASTQ files were imported to CLC Genomics Workbench (ver 10.1.1, Qiagen, Hilden, Germany). Reads were mapped to the mouse reference genome (mm10). CLC Main Workbench (ver 21.0.4, Qiagen) was used for the downstream analysis. The total counts were normalized using the scaling method. Transformed values (log_2-converted after adding 1 to the normalized expression value) were used to plot the heatmap. Low-expression genes

(normalized expression value <10 in any sample) were excluded before differential gene expression (DEG) analysis. DEG analysis was performed using the Empirical Analysis of the DGE tool with standard parameters. We selected 1001 genes with a false discovery rate p-value of < 0.05 in any pair within the three groups as significant DEGs. A heatmap of hierarchically clustered significant DEGs (Figure 3B) was plotted using Heatmapper,[44] and Metascape[45] was used for Gene Ontology analysis. The relative expression bar charts were created using GraphPad Prism software (version 8.4.3, Boston, MA, USA) with the normalized expression value as the ratio concerning the Ctrl group; the significance was described as a p-value in the results of the aforementioned DEG analysis.

Isolation of non-CMs and Tomato$^+$ cells using FACS

The isolation of non-CMs from the murine ventricles was performed as described previously.[14,28] Briefly, after mice were euthanized by CO_2 inhalation, the hearts were immediately cannulated and perfused with cold PBS (50 mL). The heart was removed for each mouse, the atria and valves were separated to isolate ventricles, and the ventricular myocardium was cut into 1-mm pieces on a Petri dish on ice. Samples were transferred into tubes with 3 mL of enzyme solution containing 2 mg/mL collagenase type IV (CLS-4; Worthington Biochemical Corporation, Lakewood, NJ, USA) and 1.2 U/mL Dispase II (255-914-4; Sigma), incubated in a 37°C water bath for 45 min, and triturated every 15 min. After filtering the enzyme/tissue mixture, debris and red blood cells were removed using Debris Removal Solution (130-109-398; Miltenyi Biotec, North Rhine-Westphalia, Germany) and RBC lysis buffer (60-00050-11; pluriSelect, Leipzig, Germany), respectively. BD FACSAria IIIu (BD, Franklin Lakes, NJ, USA) and MoFlo XDP (Beckman Coulter) were used to collect non-CMs and Tomato$^+$ cells, respectively. Non-CM sorting for single-cell RNA sequencing (scRNA-seq) was performed using Live/Dead (1:1000; L34975, Invitrogen), Calcein Violet Working

solution (0.1 μM, 425203; BioLegend, San Diego, CA, USA) to isolate cells with intact cell membranes and active metabolism (Live/Dead-, Calcein+) with minimal pressure.

scRNA-seq

Intact non-CMs from each heart (Ctrl-chow, Ctrl-HFpEF, and TTg-HFpEF; n=2, respectively) were isolated using FACS at 15 weeks. The scRNA-seq library from non-CMs was generated using a Chromium controller from 10X Genomics. Approximately 10,000 isolated non-CMs were loaded into each channel of a dedicated plate and processed using the Chromium Single Cell 3′ v3.1 reagent kit (10X Genomics, Pleasanton, CA, USA). Sequencing was performed on a NovaSeq 6000 (Illumina, San Diego, CA, USA) system operated by the Center for Omics and Bioinformatics, Graduate School of Frontier Sciences, University of Tokyo. Sequence reads were processed using the Cell Ranger v.5.0.0 pipeline from 10X Genomics to create fastq files. Briefly, de-multiplexed fastq files were aligned to a custom reference genome comprising the mm10/GRCm38 reference genome plus the Tomato sequence, and a gene expression matrix was generated using the Cellranger count pipeline. After Cellranger count processing, scRNA-seq data were analyzed using the Seurat version 4.0.1[46] in R version 4.0.3 (https://www.r-project.org/). Cells with gene expression <200 or > =5000 or >10% of reads mapped to mitochondria were excluded to remove low-quality cells. Subsequently, the expression values were normalized (NormalizeData function; scale.factor=10,000). The IntegratedData function generated an integrated Seurat object that corrected for technical differences between data sets. The dimensional reduction was performed using the Uniform Manifold Approximation and Projection (UMAP) algorithm with the RunPCA and RunUMAP functions implemented in the Seurat package. After dimensional reduction of the integrated Seurat object with dims = 1:30 and resolution = 0.25, the cell type of each cluster was identified based on gene expression as known markers. Three clusters exhibiting a low median nFeature_RNA value of <1000 and

expressing genes related to erythrocytes, platelets, and ribosomal RNA, respectively, were omitted from further examination. The DimPlot function was used for cluster visualization after dimensional compression.

For cardiac fibroblast (CF) analysis, CF clusters were extracted by subset function. After obtaining CF clusters (dims = 1:30 and resolution = 1.0), two doublet clusters expressing genes associated with endothelial and immune cells were removed. Subsequently, the data were reclustered (with the settings dims = 1:15 and resolution = 0.15) and used for downstream analysis. The average UMI counts for all CF clusters exceeded 10000. To create a cluster dendrogram for each CF cluster, we used the BuildClusterTree function, which performs estimates based on a distance matrix constructed in the PCA space. Two Seurat functions were used to identify the marker genes: the FindAllMarkers function was used to compare each cluster with other clusters, and the FindMarkers function was used to perform pairwise comparisons between groups. For each marker gene in the CF subcluster, the average fold change (avg_logFC) and Bonferron-adjusted p-value (p_val_adj) were calculated, and the top five genes in avg_logFC were selected to represent cluster-specific markers. The following Seurat functions were used to visualize the gene expression data: FeaturePlot, VlnPlot, DotPlot, and DoHeatmap. For DoHeatmap, the top 10 marker gene expressions in 200 cells per cluster are shown. For genes displayed in Vlnplot, expression values were extracted using the FetchData function and tested using the Kruskal–Wallis with Dunn's post hoc test with GraphPad Prism software. Previously reported gene sets[6,47] were used to calculate the ECM score, and the AddModuleScore function was used to calculate the average score for multiple gene groups combined. To visualize the changes in gene expression for each CF cluster in each group, we selected genes that were significantly upregulated in the Ctrl-HFpEF group compared to those in the Ctrl-chow group (p_val_adj < 0.05 and avg_logFC > 0.18), and the heatmap was created using Heatmapper[44] (Figure 4F). To calculate and visualize the intensity

of intercellular communication based on single-cell gene expression profiles, ligand receptors, and cofactors, we used the CellChat package (version 1.1.3).[48]

Spatial transcriptomics

Spatial transcriptomics was analyzed for each sample per group (Ctrl-chow, Ctrl-HFpEF, and TTg-HFpEF; n=1) at 15 weeks. Mice were euthanized by CO_2 inhalation, and the hearts were immediately cannulated and perfused with cold PBS. The hearts were removed and formalin-fixed, and paraffin-embedded (FFPE) blocks were created. Heart FFPE blocks were sectioned (5 μm) along the short-axis image at the left ventricular papillary muscle level and placed on a barcoded spot on a glass slide. cDNA libraries were prepared following the Visium Spatial Gene Expression for FFPE protocol. Sequencing was performed on a NovaSeq 6000 (Illumina) system. 10X Genomics Spaceranger v1.3.1 pipeline was used to perform sample de-multiplexing, reads alignment, and generate feature-spot matrices. The reads were aligned to the mm10/GRCm38 reference transcriptome. HE staining was supplemented with Spaceranger for tissue detection, fiducial detection, and spatial position alignment of sequenced data points.

The spatial transcriptomics data were analyzed using Seurat version 4.0.1[46] under R version 4.0.3 (https://www.r-project.org/). Gene expression data were normalized in each sample using the SCTransform function. The merge function was used to work with each sample in the same Seurat object. The SpatialFeaturePlot function was used for gene expression visualization in HE-stained images. The AddModuleScore function was used to visualize the average expression scores of the top 30 marker genes of each CF cluster in scRNA-seq.

Retrovirus infection, Sendai virus vector infection, and cell culture

MEF isolation, pMXs retroviral vector generation, and transduction with retroviruses were performed as described previously.[49] For MEF isolation, mouse embryos were isolated from

12.5-day pregnant mice euthanized by CO_2 inhalation and then washed with PBS, and the head and visceral tissues were carefully removed. These tissues were used for genotyping. Fibroblasts were isolated from the rest of the embryos. For mouse CF isolation, adult mice (older than 8 weeks of age) were euthanized by CO_2 inhalation, and their hearts were quickly removed. CFs were isolated as described above (see Isolation of non-CMs and Tomato$^+$ cells). Isolated CF pellets were resuspended for culturing in IMDM (12440-053, Gibco, Waltham, MA, USA) supplemented with 20% fetal bovine serum (FBS; CCP-FBS-BR-500 COSMO BIO, Tokyo, Japan) at 37 °C in 5% CO_2. The medium was replaced every two days. pMX-Cre vectors were transfected into Plat-E cells using Fugene 6 (E2691; Promega, Madison, WI, USA). MEFs and mouse CFs were transduced with the retrovirus as indicated. The medium was replaced with Dulbecco's Modified Eagle Medium (DMEM; 044-29765, Fujifilm Wako, Osaka, Japan)/Medium 199 (11150-059; Gibco, Waltham, MA, USA) supplemented with 20% FBS after 24 h of transduction.

Human CF (HCF) isolation, generation, and transduction of Sendai viral (SeV) vectors were performed as described previously.[15] Human atrial tissues were obtained from patients undergoing cardiac surgery with informed consent, in accordance with the Tsukuba University Ethics Committee guidelines. Cardiac tissues were minced into pieces and plated on gelatin-coated dishes to isolate HCFs. The Tsukuba Clinical Research and Development Organization approved all human experiments conducted in this study (H30-273).

Mouse CFs and HCFs were transduced with the SeV-Gata4 vectors (SeV-Gata4/TSΔF) and cultured in DMEM/Medium 199/20% FBS. Mouse CFs were transfected with 15 nM of mouse siMeox1 (SASI_Mm01_00059250, Sigma) or 15nM siRNA Control (SIC001, Sigma) using Lipofectamine RNAiMAX transfection reagent (13778-075; Thermo Fisher) according to the manufacturer's protocol. The following day, the medium was changed to IMDM/0.5% FBS supplemented with TGF-β1 (10 ng/mL; #100-21C; Peprotech, Inc, Rocky Hills, NJ, USA) and

analyzed three days later.

Neonatal rat CM culture and preparation of conditioned medium

To isolate neonatal rat CMs, the Pierce Primary Cardiomyocyte Isolation Kit (88281, Thermo Scientific) was used according to the manufacturing protocol. Briefly, day-one neonatal rats (Jcl: SD) were euthanized by decapitation, and the hearts were harvested under sterile conditions. Jcl: SD rats were purchased from CLEA Japan (Tokyo, Japan).

Adult mouse CFs transduced with or without SeV-Gata4 vector were cultured in DMEM/Medium 199/20% FBS. The following day, the medium was replaced with IMDM/0.5% FBS supplemented with TGF-β1 (10 ng/mL). After two days, all dishes were washed twice, replaced with DMEM medium containing 0.5% FBS, and incubated for 24 h. The conditioned medium was collected in a 50 mL tube through a 0.45 μm filter (17598K, Sartorius, Goettingen, Germany) and used immediately after collection and filtration. Neonatal rat CM cultures were changed to the above conditioning medium and analyzed after two days of culture.

Immunocytochemistry

For immunocytochemistry, the cells were fixed in 4% PFA for 15 min at 25°C, blocked with 5% normal goat serum blocking solution (S-1000; Vector Laboratories, Burlingame, CA), and incubated with primary antibodies against αSMA (1:400, A5228, Sigma) or α-actinin (1:800, A7811, Sigma). The cells were then incubated with secondary antibodies conjugated with Alexa 488 (1:200, A11001, Invitrogen) or Alexa Fluor 546 (1:200, A11003, Invitrogen) and counterstained with DAPI (Invitrogen, D1306). All experiments were performed using an all-in-one fluorescence microscope (BZX810; Keyence, Osaka, Japan).

αSMA intensity was measured as described previously.[7] Briefly, images were obtained in the

same acquisition settings across samples. The fold change in αSMA expression was quantified using the ImageJ software. The average fluorescence intensity of αSMA was quantified using the Measure tool and normalized to that of the total cell number. A total of 10 regions were randomly selected and analyzed per well. For analyses of CM size, CM surface area was quantified using the ImageJ software (NIH). A total of five regions of interest were analyzed per well. All measurements and calculations were performed under blinded conditions.

Public ChIP-seq data analysis

To estimate the direct binding of Gata4 to Meox1 enhancer and epigenetic status, we analyzed the published ChIP-seq data (GSM3067561)[24] for Gata4 binding and H3K27ac expression in the control and MGTH-overexpressed fibroblasts. Integrative Genomics Viewer[50] was used for peak visualization of ChIP-seq.

Quantification and statistical analysis

Statistical analyses were performed using GraphPad Prism software. The figures and figure legends report statistical parameters, including the number of samples (n), descriptive statistics (mean and standard error of the mean), and significance. In general, at least three measurements were performed for each time point and experiment. Model assumptions were checked using the Shapiro-Wilk normality test or visual inspection of residual and fitted value plots. Differences between groups were examined for statistical significance using the Student's t-test or one-way analysis of variance (ANOVA) followed by Tukey's or Dunnett's *post hoc* test. The statistical tests used in RNA-seq and scRNA-seq are described in the corresponding sections above. Two-way ANOVA with Tukey's *post hoc* test was used to assess the time series data. Differences were regarded as significant at p-values of < 0.05.

Data and code availability

All sequencing data files are available from GEO, the Super-Series reference number GSE218761. All codes have been deposited at Zenodo with a DOI of 10.5281/zenodo.7618993.

Supplementary Tables

Table S1 Study design

Study	Groups	Genotype	Sex	Age (weeks)	Number (prior to experiment)	Number (after termination)	Littermates (Yes/No)	Other description
Figure1B, S1C-D	Ctrl	Tcf21^{iCre}/Tomato	M	10–12	4	4	Yes	
	TTg	Tcf21^{iCre}/Tomato/ MGTH2A	M	10–12	4	4	Yes	
Figure1E-G, J-K Figure2B Figure S1E-H	Ctrl-Chow	Tcf21^{iCre}/Tomato	M	10–12	7	7	Yes	Chow: normal chow feeding HFpEF: HFD + L-NAME feeding
	TTg-Chow	Tcf21^{iCre}/Tomato/ MGTH2A	M	10–12	7	7	Yes	
	Ctrl-HFpEF	Tcf21^{iCre}/Tomato	M	10–12	10	10	Yes	
	TTg-HFpEF	Tcf21^{iCre}/Tomato/ MGTH2A	M	10–12	10	10	Yes	
Figure1H-I Figure2A, C-J Figure5F Figure S2E-H, S7C	Ctrl-Chow	Tcf21^{iCre}/Tomato	M	10–12	6	6	Yes	Chow: normal chow feeding HFpEF: HFD + L-NAME feeding
	TTg-Chow	Tcf21^{iCre}/Tomato/ MGTH2A	M	10–12	6	6	Yes	
	Ctrl-HFpEF	Tcf21^{iCre}/Tomato	M	10–12	6	6	Yes	
	TTg-HFpEF	Tcf21^{iCre}/Tomato/ MGTH2A	M	10–12	6	6	Yes	

Figure3, 4 Figure5A-E FigureS4, S5, S6, S7A-B	Ctrl-Chow	Tcf21^{iCre}/Tomato	M	10–12	6	6	Yes	Randomly selected mice were assigned as follows. ・RNA-seq: n=3, each ・scRNA-seq: n=2, each ・Spatial transcriptomics: n=1, each
	Ctrl-HFpEF	Tcf21^{iCre}/Tomato	M	10–12	6	6	Yes	
	TTg-HFpEF	Tcf21^{iCre}/Tomato/MGTH2A	M	10–12	6	6	Yes	
Figure6D-E, G Figure7A Figure S8B-D, F	Ctrl-Chow	Tcf21^{iCre}	M	10–12	8	8	Yes	Chow: normal chow feeding HFpEF: HFD + L-NAME feeding
	Ctrl-HFpEF	Tcf21^{iCre}	M	10–12	8	8	Yes	
	SF-G-HFpEF	Tcf21^{iCre}/SF-G	M	10–12	8	8	Yes	
	SF-M-HFpEF	Tcf21^{iCre}/SF-M	M	10–12	8	8	Yes	
	MGTH2A-HFpEF	Tcf21^{iCre}/MGTH2A	M	10–12	8	8	Yes	
Figure6H FigureS9 E-H	Ctrl-Chow	Tcf21^{iCre}	M	10–12	6	6	Yes	Chow: normal chow feeding HFpEF: HFD + L-NAME feeding
	Ctrl-HFpEF	Tcf21^{iCre}	M	10–12	6	6	Yes	
	SF-G-HFpEF	Tcf21^{iCre}/SF-G	M	10–12	6	6	Yes	
	SF-M-HFpEF	Tcf21^{iCre}/SF-M	M	10–12	6	6	Yes	
	MGTH2A-HFpEF	Tcf21^{iCre}/MGTH2A	M	10–12	6	6	Yes	

Figure6F	Ctrl-Chow	Tcf21^{iCre}	M	10–12	5	5	Yes	Chow: normal chow feeding HFpEF: HFD + L-NAME feeding
	Ctrl-HFpEF	Tcf21^{iCre}	M	10–12	5	5	Yes	
	SF-G-HFpEF	Tcf21^{iCre}/SF-G	M	10–12	5	5	Yes	
	SF-M-HFpEF	Tcf21^{iCre}/SF-M	M	10–12	5	5	Yes	
	MGTH2A-HFpEF	Tcf21^{iCre}/MGTH2A	M	10–12	5	5	Yes	
FigureS8E	Ctrl-Chow	Tcf21^{iCre}	M	10–12	6	6	Yes	
	SF-G-Chow	Tcf21^{iCre}/SF-G	M	10–12	6	6	Yes	
Figure S2A-D	Ctrl-Chow	Tcf21^{iCre}/Tomato	M	10–12	6	6	Yes	Chow: normal chow feeding HFpEF: HFD + L-NAME feeding
	TTg-Chow	Tcf21^{iCre}/Tomato/MGTH2A	M	10–12	6	6	Yes	
	Ctrl-HFpEF	Tcf21^{iCre}/Tomato	M	10–12	6	6	Yes	
	TTg-HFpEF	Tcf21^{iCre}/Tomato/MGTH2A	M	10–12	6	6	Yes	
Figure S3A	Ctrl-HFpEF	Tcf21^{iCre}/Tomato	M	10	10	10	Yes	HFpEF: HFD + L-NAME feeding
Figure S3B	Ctrl-HFpEF Day0	Tcf21^{iCre}/Tomato	M	10–12	6	6	Yes	HFpEF: HFD + L-NAME feeding
	TTg-HFpEF Day0	Tcf21^{iCre}/Tomato/MGTH2A	M	10–12	6	6	Yes	

	Ctrl-HFpEF 5W	Tcf21^{iCre}/Tomato	M	10–12	6	6	Yes	
	TTg-HFpEF 5W	Tcf21^{iCre}/Tomato/ MGTH2A	M	10–12	6	6	Yes	
	Ctrl-HFpEF 10W	Tcf21^{iCre}/Tomato	M	10–12	6	6	Yes	
	TTg-HFpEF 10W	Tcf21^{iCre}/Tomato/ MGTH2A	M	10–12	6	6	Yes	
	Ctrl-HFpEF 15W	Tcf21^{iCre}/Tomato	M	10–12	6	6	Yes	
	TTg-HFpEF 15W	Tcf21^{iCre}/Tomato/ MGTH2A	M	10–12	6	6	Yes	
Figure S9A-D	Ctrl-Chow	Tcf21^{iCre}/Tomato	M	10–12	6	6	Yes	Chow: normal chow feeding HFpEF: HFD + L-NAME feeding
	Ctrl-HFpEF	Tcf21^{iCre}/Tomato	M	10–12	6	6	Yes	
	SF-G-HFpEF	Tcf21^{iCre}/Tomato/ SF-G	M	10–12	6	6	Yes	
	SF-M-HFpEF	Tcf21^{iCre}/Tomato/ SF-M	M	10–12	6	6	Yes	
	MGTH2A-HFpEF	Tcf21^{iCre}/Tomato/ MGTH2A	M	10–12	6	6	Yes	

Table S2. TaqMan probes (Applied Biosystems) and RT-qPCR primer sequences for Universal Probe Library (Roche) (related to the Supplemental Methods).

(a) TaqMan gene expression assay (Applied Biosystems, Waltham, MA, USA)

Gene name	TaqMan probe
Col1a1	Mm00801666_g1

Col1a2	Mm00483888_m1
Col3a1	Mm01254476_m1
Fn1	Mm01256744_m1
Gata4	Mm00484689_m1
Hand2	Mm00439247_m1
Mef2c	Mm01340842_m1
Nppb	Mm01255770_g1
Postn	Mm00450111_m1
Tbx5	Mm00803518_m1
Tgfb1	Mm01178820_m1
Acta2	Hs00426835_g1
Col1a1	Hs00164004_m1
Ctgf	Hs00170014_m1
Meox1	Hs00244943_m1
Postn	Hs00170815_m1
Tgfb1	Hs00998133_m1

(b) Universal probe Library System (Roche, Basel, Switzerland)

Gene name	Primer	Universal Probe Library
Gapdh (mouse)	5′ - AGCTTGTCATCAACGGGAAG- 3′	#9
	5′ - TTTGATGTTAGTGGGGTCTCG- 3′	
Gapdh (human)	5′ -AGCCACATCGCTCAGACAC- 3′	#60
	5′ -GCCCAATACGACCAAATCC- 3′	

Table S3. Mouse genotyping PCR primers (related to METHODS).

Name	Sequence
CAT-forward	5′ -CAGTCAGTTGCTCAATGTACC-3′
CAT-reverse	5′ -ACTGGTGAAACTCACCCA-3′

Cre-forward	5′ -GTTCGCAAGAACCTGATGGACA-3′
Cre-reverse	5′ -CTAGAGCCTGTTTTGCACGTTC-3′
Tomato-forward	5′ -CTGTTCCTGTACGGCATGG-3′
Tomato-reverse	5′ -GGCATTAAAGCAGCGTATCC-3′
SF_insert-forward	5′ -ATGCCCTGGCTCACAAATAC-3′
SF_insert-reverse	5′ -GCCAACCTTTGTTCATGGCA-3′
SF_donor_Tg-forward	5′ -TTGCCGGGAAGCTAGAGTAA-3′
SF_donor_Tg-reverse	5′ -TTTGCCTTCCTGTTTTTGCT-3′
SF_Rosa5′ check_Tg-forward	5′ -TCTTTTCTGTTGGACCCTTACCTTGACC-3′
SF_Rosa5′ check_Tg-reverse	5′ -ACGTCAATGGAAAGTCCCTATTGGCGTTAC-3′
SF_Rosa3′ check_Tg-forward	5′ -TGCCATGAACAAAGGTTGGCTATAAAGA-3′
SF_Rosa3′ check_Tg-	5′ -

reverse	AGGATAGTGCAGGGAAACCCAAAGAAGT- 3′

Figure S1

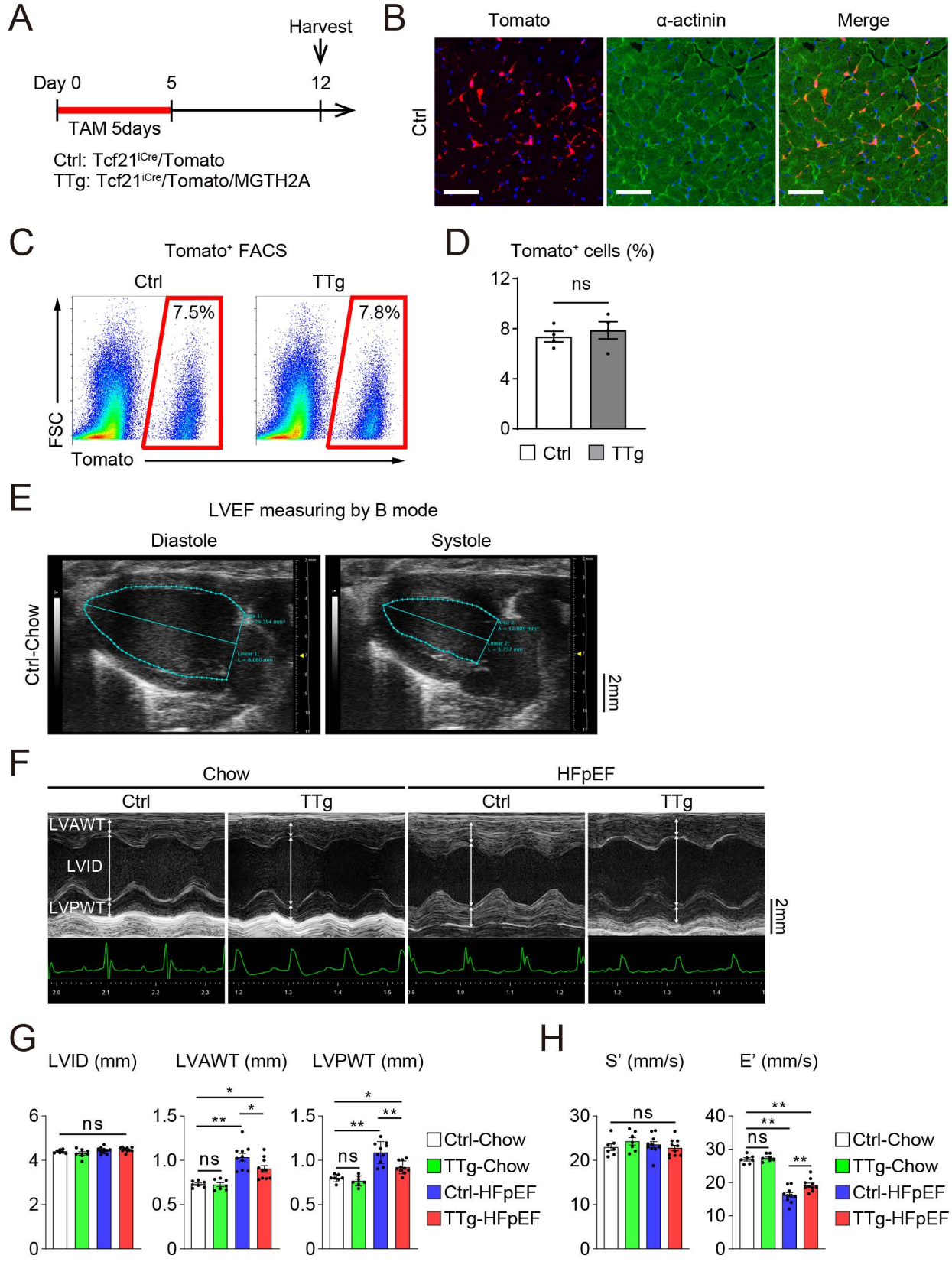
A
Harvest
Day 0
5
12
TAM 5days
Ctrl: Tcf21iCre/Tomato
TTg: Tcf21iCre/Tomato/MGTH2A
B
Tomato
α-actinin
Merge
Ctrl
C
Tomato+ FACS
Ctrl
TTg
7.5%
7.8%
FSC
Tomato
D
Tomato+ cells (%)
ns
Ctrl
TTg
E
LVEF measuring by B mode
Diastole
Systole
Ctrl-Chow
2mm
F
Chow
HFpEF
Ctrl
TTg
Ctrl
TTg
LVAWT
LVID
LVPWT
2mm
G
LVID (mm)
LVAWT (mm)
LVPWT (mm)
ns
Ctrl-Chow
TTg-Chow
Ctrl-HFpEF
TTg-HFpEF
H
S' (mm/s)
E' (mm/s)
ns
Ctrl-Chow
TTg-Chow
Ctrl-HFpEF
TTg-HFpEF

Figure S2

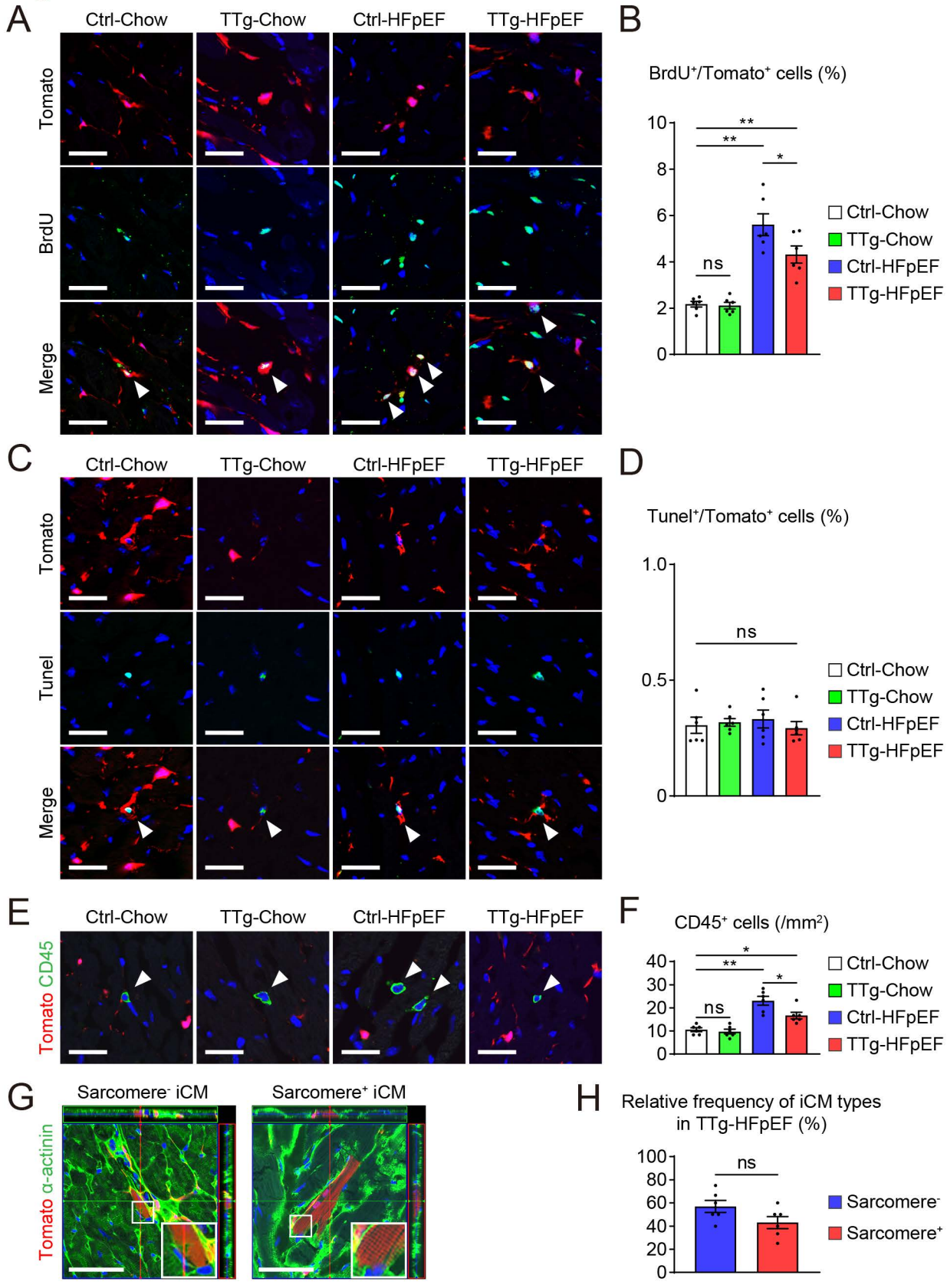
A
Ctrl-Chow
TTg-Chow
Ctrl-HFpEF
TTg-HFpEF
Tomato
BrdU
Merge
B
BrdU+/Tomato+ cells (%)
10
8
6
4
2
0
**
**
*
ns
Ctrl-Chow
TTg-Chow
Ctrl-HFpEF
TTg-HFpEF
C
Ctrl-Chow
TTg-Chow
Ctrl-HFpEF
TTg-HFpEF
Tomato
Tunel
Merge
D
Tunel+/Tomato+ cells (%)
1.0
0.5
0
ns
Ctrl-Chow
TTg-Chow
Ctrl-HFpEF
TTg-HFpEF
E
Ctrl-Chow
TTg-Chow
Ctrl-HFpEF
TTg-HFpEF
Tomato CD45
F
CD45+ cells (/mm2)
40
30
20
10
0
*
**
*
ns
Ctrl-Chow
TTg-Chow
Ctrl-HFpEF
TTg-HFpEF
G
Sarcomere- iCM
Sarcomere+ iCM
Tomato α-actinin
H
Relative frequency of iCM types
in TTg-HFpEF (%)
100
80
60
40
20
0
ns
Sarcomere-
Sarcomere+

Figure S3

A

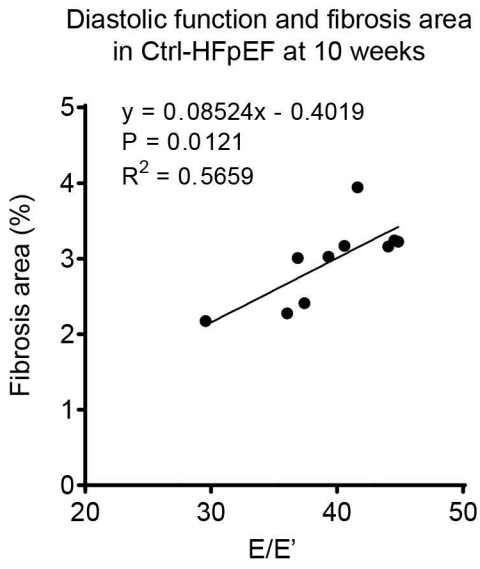
Diastolic function and fibrosis area
in Ctrl-HFpEF at 10 weeks
y = 0.08524x - 0.4019
P = 0.0121
R2 = 0.5659
Fibrosis area (%)
E/E'
0
1
2
3
4
5
20
30
40
50

B

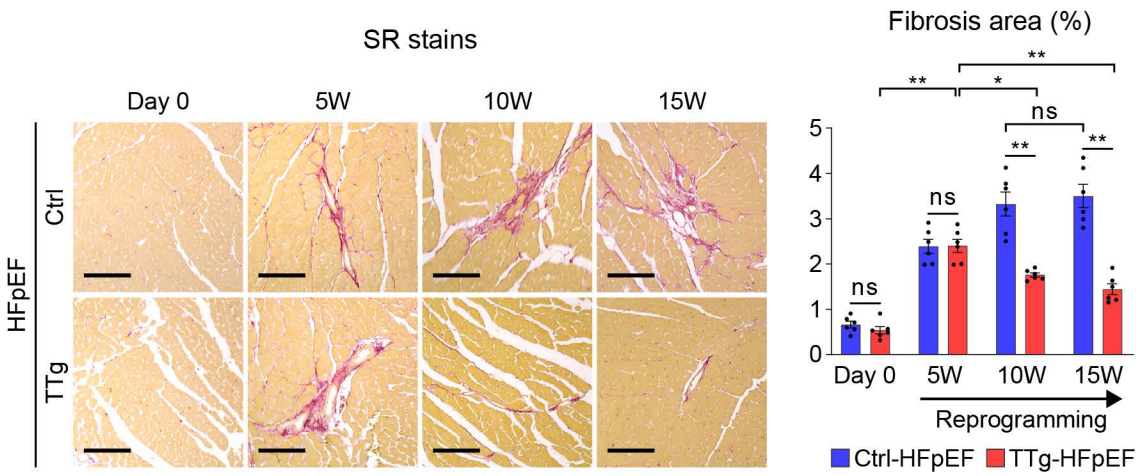
SR stains
Day 0
5W
10W
15W
HFpEF
Ctrl
TTg
Fibrosis area (%)
ns
**
*
Day 0
5W
10W
15W
Reprogramming
Ctrl-HFpEF
TTg-HFpEF

Figure S4

A

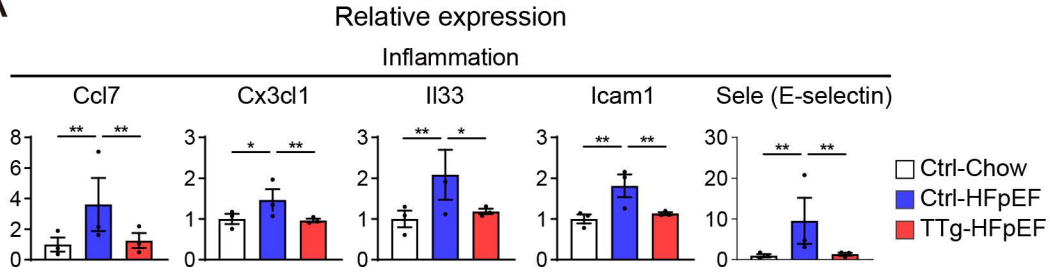
Relative expression
Inflammation
Ccl7
Cx3cl1
Il33
Icam1
Sele (E-selectin)
Ctrl-Chow
Ctrl-HFpEF
TTg-HFpEF

B

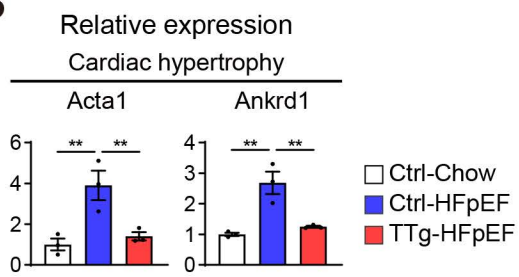
Relative expression
Cardiac hypertrophy
Acta1
Ankrd1
Ctrl-Chow
Ctrl-HFpEF
TTg-HFpEF

Figure S5

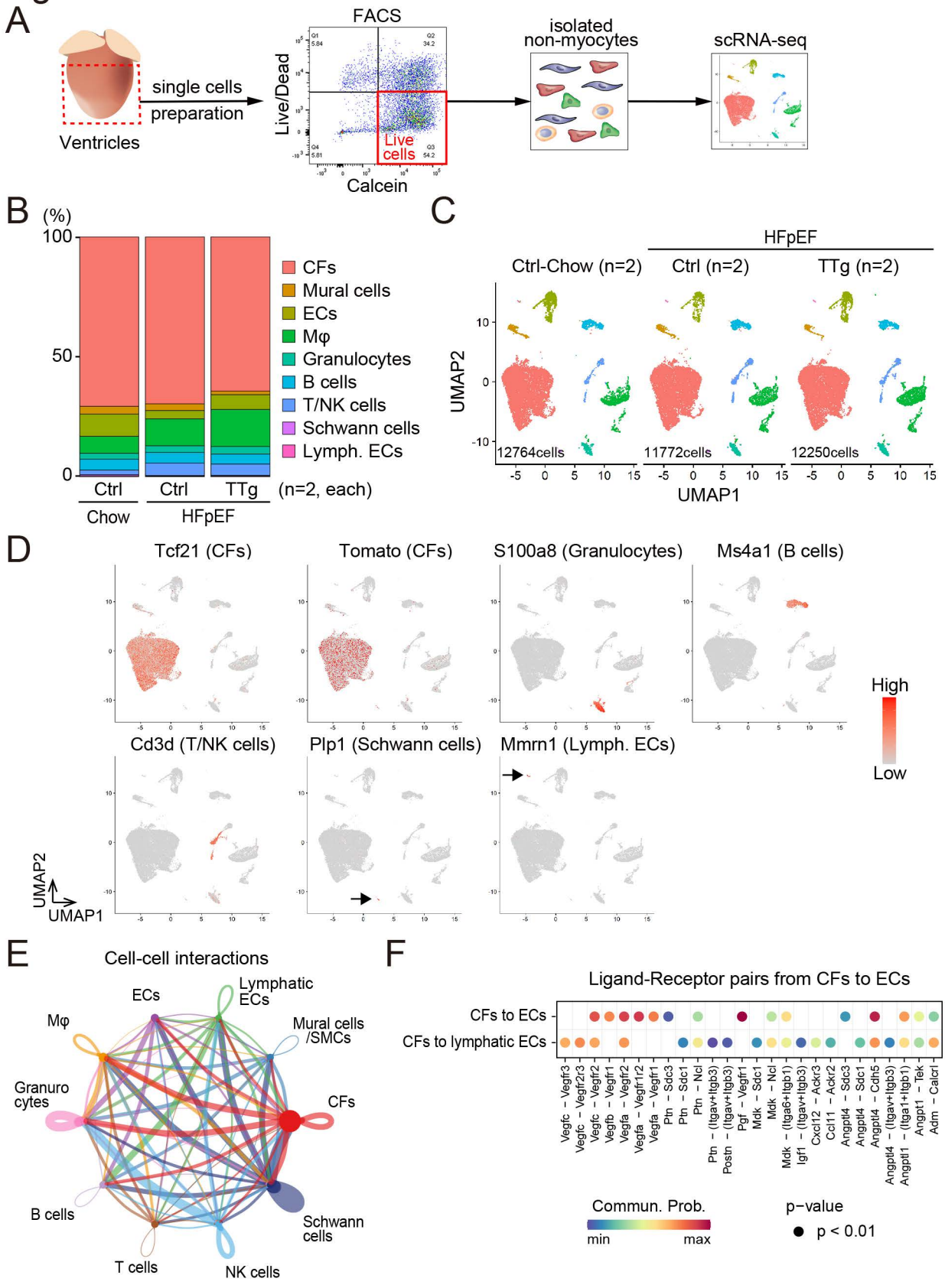
A
Ventricles
single cells
preparation
FACS
Live/Dead
Calcein
Live cells
isolated non-myocytes
scRNA-seq
B
(%)
100
50
0
Ctrl
Ctrl
TTg
Chow
HFpEF
(n=2, each)
CFs
Mural cells
ECs
Mφ
Granulocytes
B cells
T/NK cells
Schwann cells
Lymph. ECs
C
HFpEF
Ctrl-Chow (n=2)
Ctrl (n=2)
TTg (n=2)
UMAP2
UMAP1
12764cells
11772cells
12250cells
D
Tcf21 (CFs)
Tomato (CFs)
S100a8 (Granulocytes)
Ms4a1 (B cells)
Cd3d (T/NK cells)
Plp1 (Schwann cells)
Mmrn1 (Lymph. ECs)
High
Low
UMAP2
UMAP1
E
Cell-cell interactions
ECs
Lymphatic ECs
Mφ
Mural cells /SMCs
Granuro cytes
CFs
B cells
Schwann cells
T cells
NK cells
F
Ligand-Receptor pairs from CFs to ECs
CFs to ECs
CFs to lymphatic ECs
Vegfc – Vegfr3
Vegfc – Vegfr2r3
Vegfc – Vegfr2
Vegfb – Vegfr1
Vegfa – Vegfr2
Vegfa – Vegfr1r2
Vegfa – Vegfr1
Ptn – Sdc3
Ptn – Sdc1
Ptn – Ncl
Ptn – (Itgav+Itgb3)
Postn – (Itgav+Itgb3)
Pgf – Vegfr1
Mdk – Sdc1
Mdk – Ncl
Mdk – (Itga6+Itgb1)
Igf1 – (Itgav+Itgb3)
Cxcl12 – Ackr3
Ccl11 – Ackr2
Angptl4 – Sdc3
Angptl4 – Sdc1
Angptl4 – Cdh5
Angptl4 – (Itgav+Itgb3)
Angptl1 – (Itga1+Itgb1)
Angpt1 – Tek
Adm – Calcrl
Commun. Prob.
min
max
p-value
p < 0.01

Figure S6

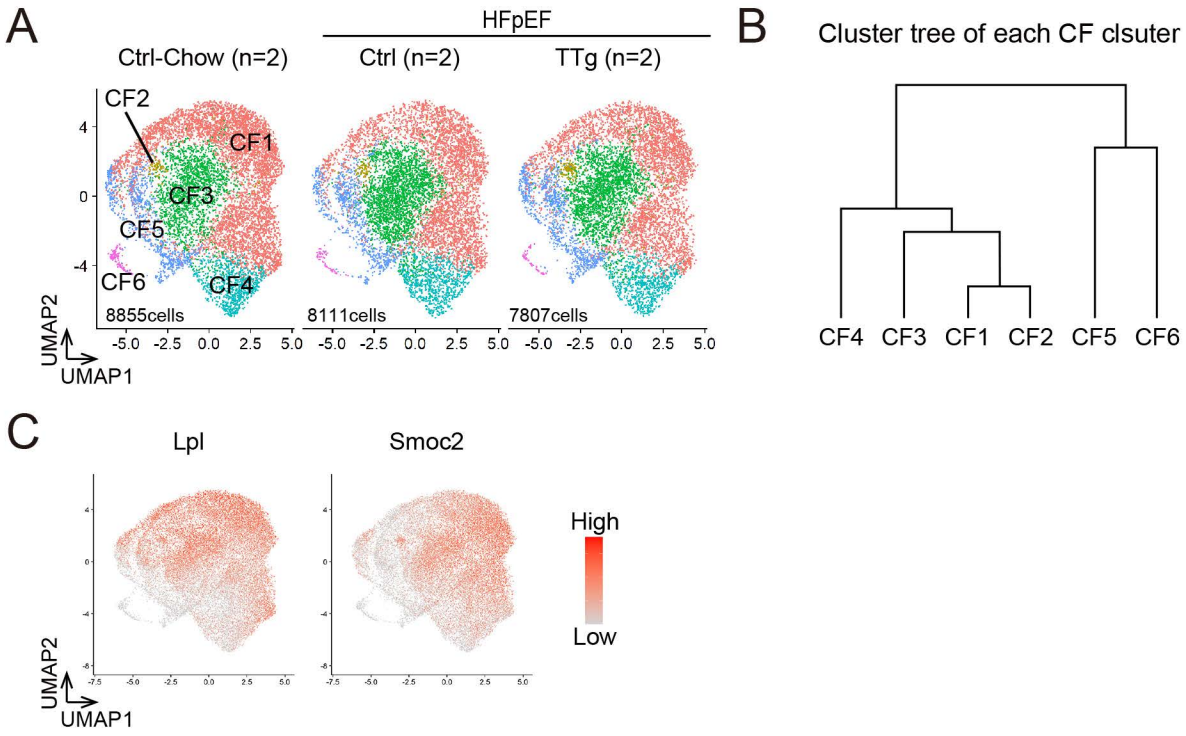
A
HFpEF
Ctrl-Chow (n=2)
Ctrl (n=2)
TTg (n=2)
CF2
CF1
CF3
CF5
CF6
CF4
8855cells
8111cells
7807cells
UMAP2
UMAP1
B
Cluster tree of each CF clsuter
CF4 CF3 CF1 CF2 CF5 CF6
C
Lpl
Smoc2
High
Low
UMAP2
UMAP1

Figure S7

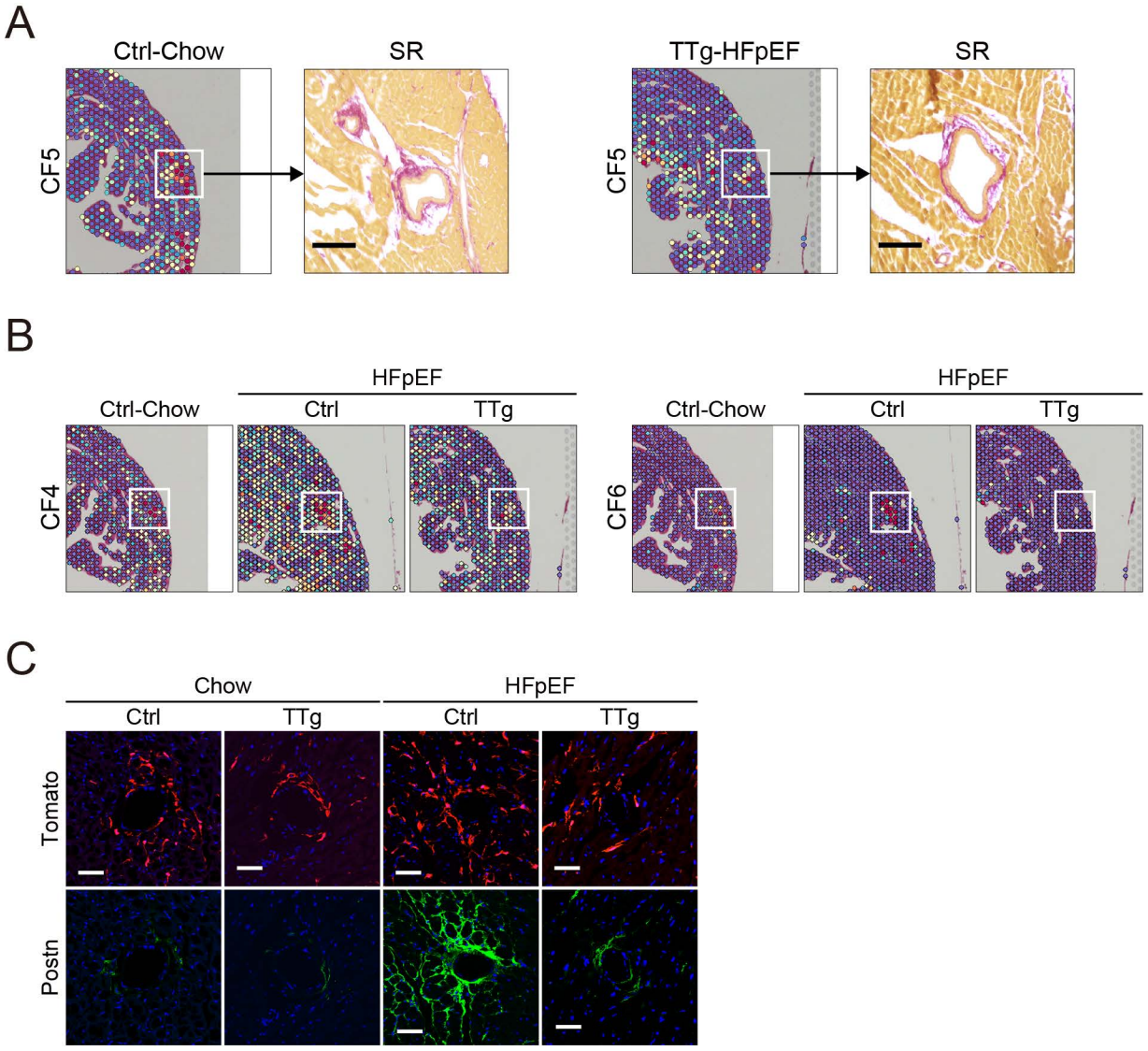
A
Ctrl-Chow
SR
TTg-HFpEF
SR
CF5
CF5
B
HFpEF
Ctrl-Chow
Ctrl
TTg
HFpEF
Ctrl-Chow
Ctrl
TTg
CF4
CF6
C
Chow
HFpEF
Ctrl
TTg
Ctrl
TTg
Tomato
Postn

Figure S8

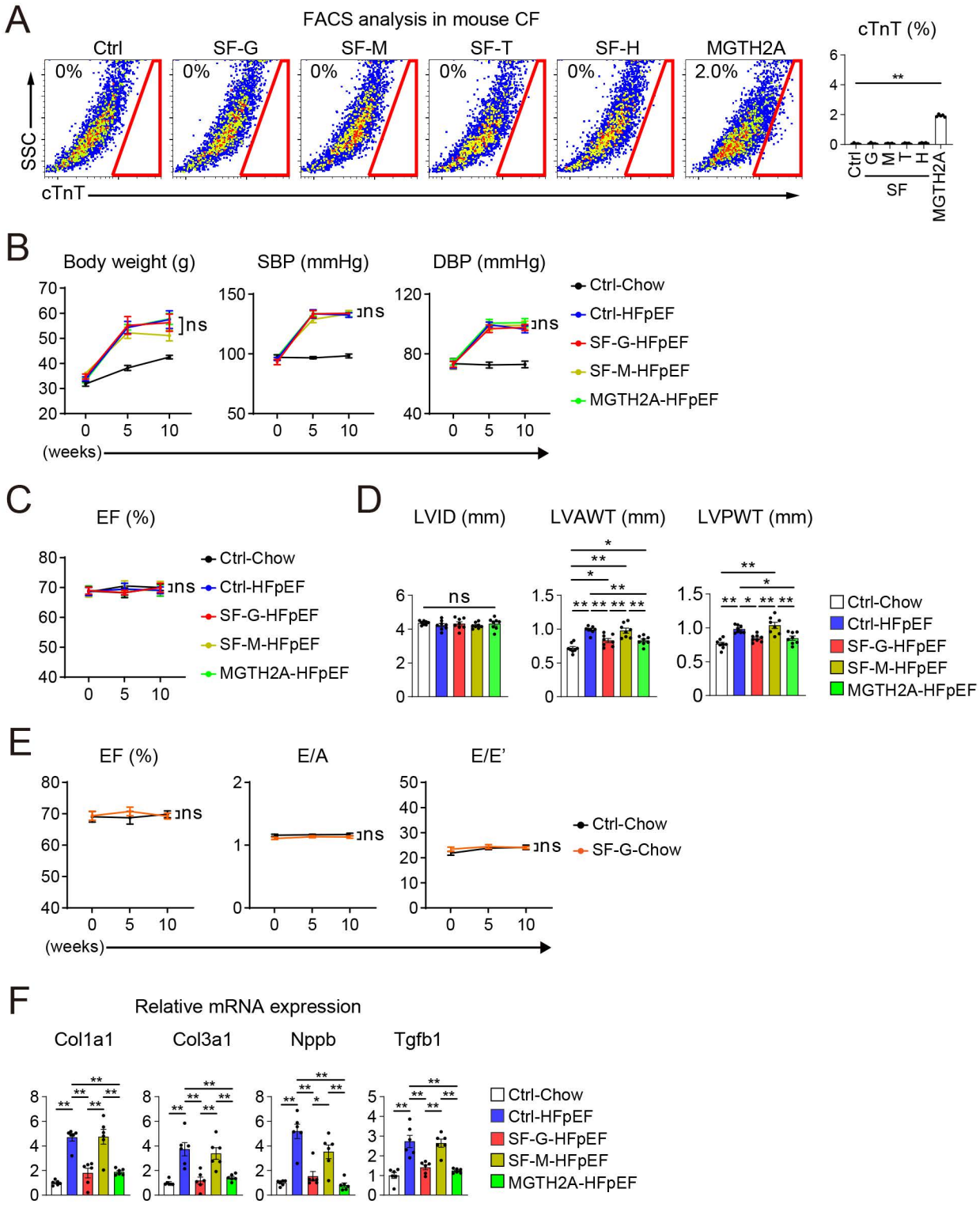
A
FACS analysis in mouse CF
Ctrl
SF-G
SF-M
SF-T
SF-H
MGTH2A
0%
0%
0%
0%
0%
2.0%
SSC
cTnT
cTnT (%)
Ctrl
G
M
T
H
SF
MGTH2A
B
Body weight (g)
SBP (mmHg)
DBP (mmHg)
ns
(weeks)
Ctrl-Chow
Ctrl-HFpEF
SF-G-HFpEF
SF-M-HFpEF
MGTH2A-HFpEF
C
EF (%)
D
LVID (mm)
LVAWT (mm)
LVPWT (mm)
E
EF (%)
E/A
E/E'
(weeks)
Ctrl-Chow
SF-G-Chow
F
Relative mRNA expression
Col1a1
Col3a1
Nppb
Tgfb1

Figure S9

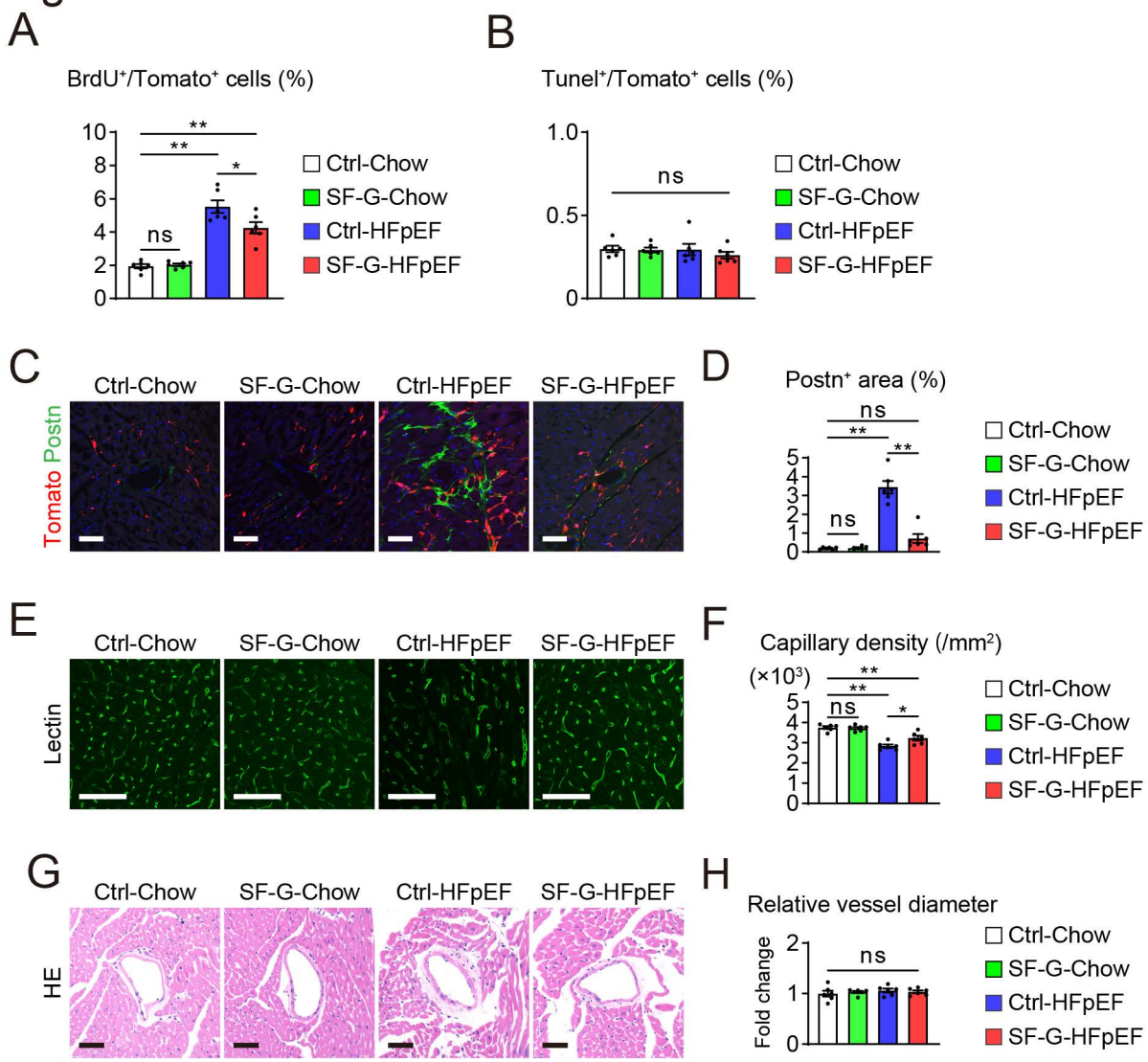
A
BrdU+/Tomato+ cells (%)
10
8
6
4
2
0
**
**
*
ns
Ctrl-Chow
SF-G-Chow
Ctrl-HFpEF
SF-G-HFpEF
B
Tunel+/Tomato+ cells (%)
1.0
0.5
0
ns
Ctrl-Chow
SF-G-Chow
Ctrl-HFpEF
SF-G-HFpEF
C
Ctrl-Chow
SF-G-Chow
Ctrl-HFpEF
SF-G-HFpEF
Tomato Postn
D
Postn+ area (%)
ns
**
**
ns
5
4
3
2
1
0
Ctrl-Chow
SF-G-Chow
Ctrl-HFpEF
SF-G-HFpEF
E
Ctrl-Chow
SF-G-Chow
Ctrl-HFpEF
SF-G-HFpEF
Lectin
F
Capillary density (/mm2)
(×103)
**
**
ns
*
5
4
3
2
1
0
Ctrl-Chow
SF-G-Chow
Ctrl-HFpEF
SF-G-HFpEF
G
Ctrl-Chow
SF-G-Chow
Ctrl-HFpEF
SF-G-HFpEF
HE
H
Relative vessel diameter
Fold change
2
1
0
ns
Ctrl-Chow
SF-G-Chow
Ctrl-HFpEF
SF-G-HFpEF

Figure S10

A

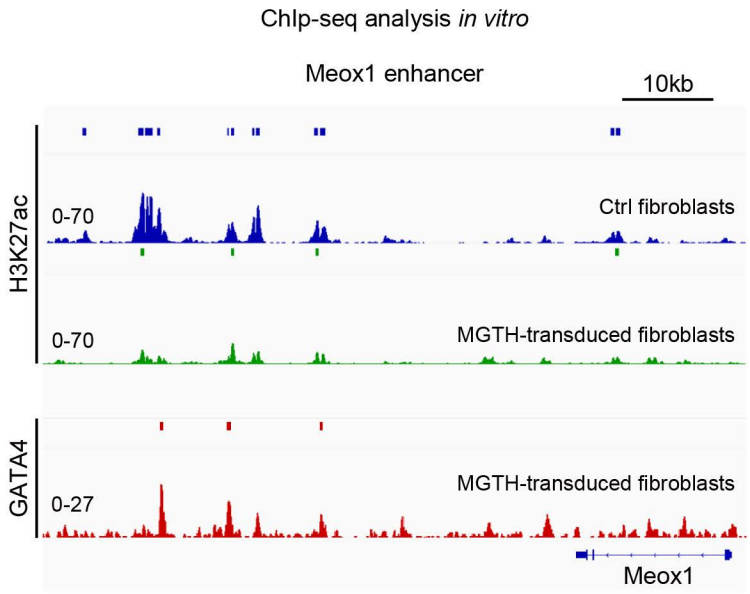

B

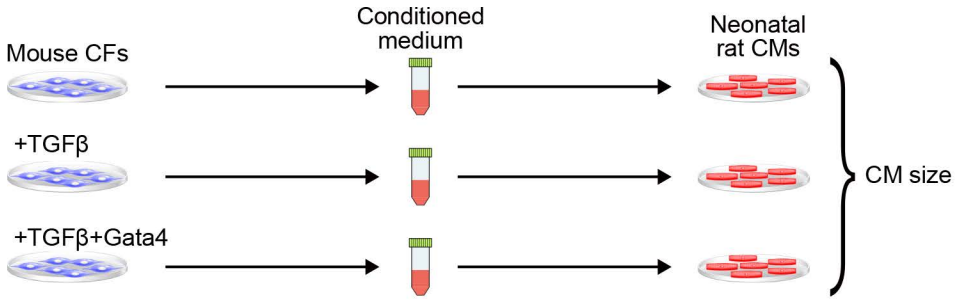

C

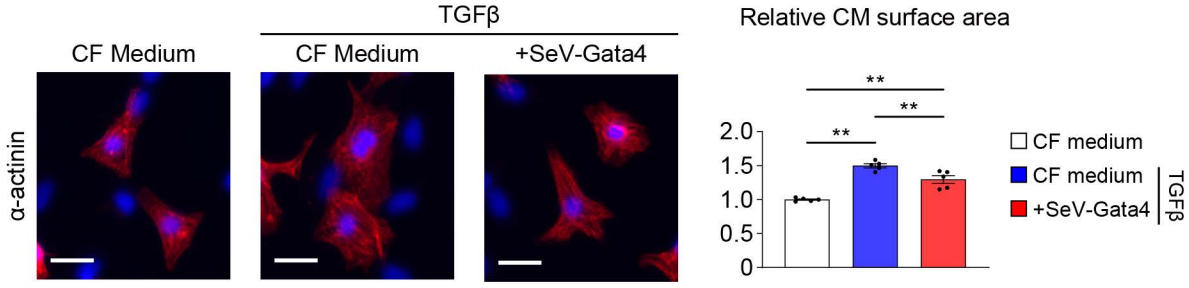

Supplemental Figure Legends

Figure S1. Cardiac reprogramming improves diastolic dysfunction in HFpEF

(A) Experimental scheme for lineage tracing of Tcf21-expressing cells *in vivo* for five consecutive days with tamoxifen (TAM) administration. Hearts were harvested seven days after TAM administration in the control littermates (Ctrl, $Tcf21^{iCre}$/Tomato) and TTg mice ($Tcf21^{iCre}$/Tomato/MGTH2A).

(B) Immunohistochemistry for Tomato, α-actinin, and DAPI expression in Ctrl mice seven days after TAM administration.

(C, D) $Tomato^{+}$ cells were collected by fluorescence-activated cell sorting (FACS) in Ctrl and TTg mice seven days after the last TAM administration. Quantitative analysis is shown in (D) (n=4 independent biological replicates).

(E) Representative images of the left ventricular ejection fraction (LVEF) measurement by B mode in echocardiography. LVEF was calculated by tracing the endocardial border around the left ventricular cavity at the end of both systole and diastole.

(F) Representative images of left ventricular measurement by M-mode in echocardiography. Arrows indicate the left ventricular anterior wall thickness (LVAWT), left ventricular internal diameter (LVID), and left ventricular posterior wall thickness (LVPWT) in the diastole.

(G) Quantitative analyses for LVID, LVAWT, and LVPWT (Ctrl-chow n=7; TTg-chow n=7; Ctrl-HFpEF; n=10, TTg-HFpEF; n=10).

(H) Quantitative analyses for S' wave and E' wave (Ctrl-chow n=7; TTg-chow n=7; Ctrl-HFpEF; n=10, TTg-HFpEF; n=10).

All data are presented as the mean ± SEM. ns; not significant, $*p < 0.05$, $**p < 0.01$; vs. the relevant control by t-test (D) and one-way ANOVA followed by Tukey's multi−comparisons test (G and H). Scale bars represent 50 μm.

HFpEF, heart failure with preserved ejection fraction; SEM, standard error of the mean

Figure S2. Cardiac reprogramming suppresses cardiac fibroblast proliferation and inflammatory cell infiltration in HFpEF

(A, B) Immunohistochemistry for Tomato, 5-bromo-2'-deoxyuridine (BrdU), and DAPI staining of the left ventricle at 15 weeks (A). Arrowheads indicate $BrdU^+$ CFs. Quantitative analysis of $BrdU^+/Tomato^+$ cells is shown in (B) (n=6 independent biological replicates).

(C, D) Immunohistochemistry of the left ventricle for Tomato, Tunel staining, and DAPI at 15 weeks (C). Arrowheads indicate $Tunel^+$ CFs. Quantitative analysis of $Tunel^+/Tomato^+$ cells is shown in (D) (n=6 independent biological replicates).

(E, F) Immunohistochemistry of the left ventricle for Tomato, CD45, and DAPI staining at 15 weeks (E). Quantitative analysis of $CD45^+$ cells is shown in (F) (n=6 independent biological replicates).

(G, H) Representative Z-stack images of Tomato and α-actinin double-positive iCMs with and without sarcomeres. Quantitative analysis for the relative frequency of iCM maturation in TTg-HFpEF is shown in (H) (n=6 independent biological replicates).

All data are presented as the mean ± SEM. ns; not significant, $*p < 0.05$, $**p < 0.01$; vs. the relevant control by one-way ANOVA followed by Tukey's multi−comparisons test (B, D, F) and t-test (H). Scale bars represent 25 μm (A, C, and E) and 50 μm (G).

HFpEF, heart failure with preserved ejection fraction; iCMS, induced cardiomyocytes; SEM, standard error of the mean

Figure S3. Cardiac fibrosis correlates with diastolic dysfunction in HFpEF

(A) Scatter plot analyzing the correlation between the E/E' ratio and fibrosis area in sections subjected to Sirius red (SR) staining in Ctrl-HFpEF at 10 weeks (n=10 independent biological

replicates).

(B) SR staining was performed to determine the fibrosis area. Time course of SR staining in Ctrl-HFpEF and TTg-HFpEF. Quantitative analysis of the fibrosis area is shown (n=6 independent biological replicates).

All data are presented as the mean ± SEM. ns; not significant, *p < 0.05, **p < 0.01; vs. the relevant control by two-way ANOVA followed by Tukey's multi−comparisons test. Scale bars represent 100 μm.

HFpEF, heart failure with preserved ejection fraction; SEM, standard error of the mean.

Figure S4. Cardiac reprogramming reduces inflammation in HFpEF hearts

(A, B) Relative mRNA expression of inflammation- (A) and cardiac hypertrophy- (B) related genes in bulk RNA-sequencing data.

All data are presented as the mean ± SEM. *p < 0.05, **p-value <0.01, Empirical analysis of differential gene expression in bulk RNA-sequencing.

HFpEF, heart failure with preserved ejection fraction; SEM, standard error of the mean.

Figure S5. Single-cell RNA sequencing in HFpEF and after cardiac reprogramming

(A) Experimental workflow and analysis for scRNA-seq. For live cell sorting, cells with intact cell membranes and active metabolism (Live/Dead-, Calcein+) were sorted.

(B, C) Uniform manifold approximation and projection (UMAP) of scRNA-seq data of non-CMs in each group (n=2, C). A bar plot of the percentage of cluster contributions is shown (B).

(D) Non-CM marker gene and Tomato expression visualized on UMAP plots.

(E) Circle plot of cell-cell ligand-receptor interactions of non-CMs by CellChat analysis. The line thickness is proportional to the total interaction strength.

(F) Significant ligand-receptor pairs from CFs to ECs in CellChat analysis. The dot color

reflects communication probabilities, and the dot size represents calculated p-values.

CFs, cardiac fibroblasts; CMs, cardiomyocytes; ECs, endothelial cells; HFpEF, heart failure with preserved ejection fraction; SEM, standard error of the mean.

Figure S6. Characterization of six CF clusters

(A) UMAP of CFs colored by clusters in Ctrl-chow, Ctrl-HFpEF, and TTg-HFpEF mice (n=2 ventricles).

(B) Transcriptome-based hierarchical clustering dendrogram of six CF subclusters. In particular, CF1–4 and CF5, 6 were distinct.

(C) Expression of representative markers of quiescent/steady-state fibroblasts as visualized on UMAP plots.

CFs, cardiac fibroblasts; HFpEF, heart failure with preserved ejection fraction; UMAP, Uniform Manifold Approximation and Projection.

Figure S7. Cardiac reprogramming suppresses POSTN expression in the perivascular areas in HFpEF

(A) Comparison of CF5 marker gene expression using spatial transcriptomics and cardiac fibrosis area by Sirius red (SR) staining in Ctrl-Chow and TTg-HFpEF mice. Sequential sections from those subjected to spatial transcriptomics were used. See also Figure 5E.

(B) Magnified images of CF4 and CF6 marker gene expression. The white box indicates the perivascular region, as shown in Figure S7A. See also Figure 5D.

(C) Immunohistochemistry of Tomato, POSTN, and DAPI in Ctrl-chow, TTg-chow, Ctrl-HFpEF, and TTg-HFpEF mouse hearts at 15 weeks. See also Figure 5F.

Scale bars represent 100 μm (A) and 50 μm (C).

HFpEF, heart failure with preserved ejection fraction.

Figure S8. Gata4 overexpression induces anti-fibrotic effects without generating iCMs

(A) FACS analysis for cardiac troponin T (cTnT) expression in adult mouse CFs transduced with pMX-Cre after one week. Quantitative data are shown (n=5 independent biological replicates).

(B) Body weight, SBP, and DBP were measured every 5 weeks for up to 10 weeks (n=8 independent biological replicates).

(C) EF was serially quantified by echocardiography in the indicated groups (n=8 independent biological replicates).

(D) Quantitative analyses for LVID, LVAWT, and LVPWT (n=8 independent biological replicates).

(E) Echocardiographic measurements of the EF, E/A ratio, and E/E' ratio in Ctrl-chow (black line, n=6) and SF-G-chow (orange line, n=6) mice.

(F) Relative mRNA expression levels of fibrosis- and heat failure-related genes in the left ventricle were detected by RT-qPCR (n=6 independent biological replicates).

All data are presented as the mean ± SEM. ns; not significant, *$p < 0.05$, **$p < 0.01$; vs. the relevant control by one-way ANOVA followed by Dunnett's multi−comparisons test (A), two-way ANOVA followed by Tukey's multi−comparisons test (B, C, E), and one-way ANOVA followed by Tukey's multi−comparisons test (D and F).

DBP, diastolic blood pressure; EF, ejection fraction; FACS, fluorescence-activated cell sorting; HFpEF, heart failure with preserved ejection fraction; iCMS, induced cardiomyocytes; LVAWT, left ventricular anterior wall thickness; LVID, left ventricular internal diameter; LVPWT, left ventricular posterior wall thickness; SBP, systolic blood pressure; SEM, standard error of the mean; RT-qPCR, reverse transcription-quantitative PCR.

Figure S9. Gata4 overexpression ameliorates histopathological changes in HFpEF

(A) Quantitative analysis of $BrdU^+/Tomato^+$ cells in the indicated groups is shown (n=6 independent biological replicates).

(B) Quantitative analysis of $Tunel^+/Tomato^+$ cells in the indicated groups is shown (n=6 independent biological replicates).

(C, D) Immunohistochemistry for Tomato, Postn, and DAPI staining of the left ventricle at 10 weeks (C). Quantitative analysis of the $Postn^+$ area is shown in (D) (n=6 independent biological replicates).

(E, F) Immunohistochemistry for Isolectin B4 (Lectin) staining of the left ventricle at 10 weeks (E). Quantitative analysis of capillary density is shown in (F) (n=6 independent biological replicates).

(G, H) Representative images of hematoxylin-eosin (HE) staining of the left ventricle at 10 weeks (G). Quantitative analysis of relative vessel diameter is shown in (H) (n=6 independent biological replicates).

All data are presented as the mean ± SEM. ns; not significant, *$p < 0.05$, **$p < 0.01$; vs. the relevant control by one-way ANOVA followed by Tukey's multi−comparisons test. Scale bars represent 50 μm (C, E, G).

HFpEF, heart failure with preserved ejection fraction; SEM, standard error of the mean.

Figure S10. Gata4 overexpression inhibits CF-induced CM hypertrophy

(A) Mouse *Meox1* locus from public ChIP–seq data (GSE112315) for *H3K27ac* and *GATA4* in the control (Ctrl) and MGTH-transduced fibroblasts. *H3K27ac* expression at the enhancer region in *Meox1* is reduced upon *MGTH* overexpression. *Gata4* peaks (binding sites) overlap with regions of *H3K27ac* repression in MGTH-transduced fibroblasts.

(B) Schematic diagram illustrating conditioned medium collection from CFs treated with the

indicated conditions. Neonatal rat CMs were cultured with the CF-conditioned media for two days and analyzed for CM hypertrophy using the ImageJ software (C).

(C) Immunofluorescence staining of α-actinin in neonatal rat CMs. Quantitative analysis of relative CM surface area is shown (n=5 independent biological replicates).

All data are presented as the mean ± SEM. ns; not significant, **$p < 0.01$; vs. the relevant control by one-way ANOVA followed by Tukey's multi−comparisons test. Scale bars represent 25 μm.

CFs, cardiac fibroblasts; CMs, cardiomyocytes; SEM, standard error of the mean.